ChemComm

Check for updates

Precise macroscopic supramolecular assembly of photopatterned hydrogels†

Yuan Xue, Kai Ye, Xuebin Wang, Yanxing Xiang, Shihao Pang, Chunyan Bao ⓘ * and Linyong Zhu ⓘ *

Here we demonstrate that a precise macroscopic supramolecular assembly (MSA) can be achieved using a surface photopatterning strategy. The electrostatic interaction of the photopatterned polyelectrolytes drives hydrogel cuboids to form a stable MSA on a millimeter scale and the spatial controllability of light enables the hydrogels to be assembled into complex supramolecular architectures.

Recently, a new self-assembly beyond the molecular level, that is macroscopic supramolecular assembly (MSA),[1] has aroused great interest due to its potential applications in microelectronics,[2] bio-adhesion,[3] and tissue scaffolds.[4] Unlike the simple supramolecular recognition between one or some interactive pairs, the assembly mechanism of MSAs is a much more complex surface–surface multivalent process. Hydrogels are usually selected as the building blocks to construct MSAs due to their flowable characteristics that can reduce surface roughness and improve the mobility of surface molecules. By means of doping and surface modification, hydrogels can achieve micro or millimetre level MSAs with the help of electrostatic attraction,[5] host–guest recognition,[6] hydrophilic–hydrophobic interactions[7] and other supramolecular interactions.[8]

However, most MSA hydrogel assemblies have the problem of a low degree of order in the contact area, angle and direction, which greatly limits their practical use as bulky supramolecular materials.[1c] For example, in order to obtain a well-defined tissue engineering scaffold, it is necessary to make the building blocks controllable.[9] Shi *et al.* applied the strategy of "interactive distance matching size of building blocks" to improve the matching degree of MSA elastomers or hydrogels, in which long range interactive forces drive the selective assembly between the building blocks and short supramolecular interactions stabilize the ordered structures.[10] Other groups used
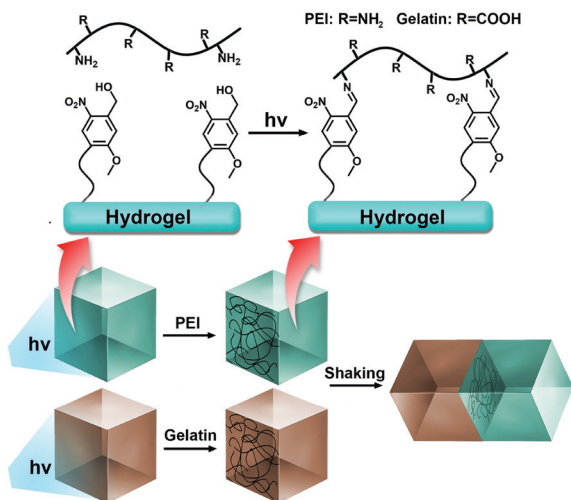
Key Laboratory of Functional Materials Chemistry, School of Chemistry & Molecular Engineering, East China University of Science and Technology, 130# Meilong Road, Shanghai 200237, China. E-mail: baochunyan@ecust.edu.cn, Linyongzhu@ecust.edu.cn

† Electronic supplementary information (ESI) available: Materials, synthesis procedures and characterization of compounds. See DOI: 10.1039/d1cc03428f

specific non-covalent interactions[11] or external forces[12] to reduce the mismatch of the shape-controlled hydrogels units. Moreover, Khademhosseini *et al.* used face-specific DNA glues to obtain diverse MSA structures in interfacial agitation systems using surface chemistry.[13] It required two rounds of hydrogel crosslinking and the operation is relatively complicated.

Alternatively, photopatterning is a widely used chemical method to construct heterogeneous surfaces, it achieves spatiotemporal resolution through non-physical contact modes and has become the preferred method for controllable modification of hydrogel surfaces.[14] Herein, we report an electrostatic-directed precise MSA by photopatterning hydrogel units (as illustrated in Scheme 1), in which photoligation chemistry of *o*-nitrobenzyl derivatives (**MNB**) is applied to immobilize the electropositive polyethylenimine (PEI) and the electronegative proteins on the hydrogel surface as desired through the coupling of the photogenerated active aldehydes of **MNB** with the amines of PEI or the proteins. Then, simply shaking in water leads to hydrogel assembly through electrostatic interactions, and diverse structures, including dimers, a linear chain of extended length and teddy bear heads, can be achieved by combing programmable photopatterning. We envision that the surface photopatterning strategy may provide a promising route to produce complex MSAs with advanced hierarchical structures.

Firstly, the photoresponsive molecule **MNB** was synthesized (Fig. S1, see the ESI†), and the structure was verified using magnetic resonance spectra and mass spectra (Fig. S2, see the ESI†). The photolysis of **MNB** was measured using a UV-Vis spectrophotometer and HPLC (Fig. S3–S5, see the ESI†), which indicated a rapid and efficient photolysis of **MNB** upon irradiation with a 365 nm LED (10 mW cm^{-2}). The mass spectra confirmed the generation of the aldehyde photoproduct accompanying the consumption of **MNB** upon irradiation. Our previous studies have shown that this photogenerated aldehyde group can effectively couple with the free amino groups of proteins[14a] and macromolecules.[15] This provides a prerequisite for the realization of controllable surface modifications of amino-containing polyelectrolytes by introducing **MNB** into the hydrogel.

Scheme 1 Schematic presentation of a precise MSA using photopatterned hydrogel units.

Fig. 1 Photoligation on microgels. (a) Schematic representation of the photoligation of PEI and gelatin on microgels. (b) The evolution of surface zeta potential of the microgels after photoligation and subsequent electrostatic adsorption.

Fig. 2 MSA of microgels and hydrogel cuboids. (a) MSA of FITC-PEI photoligated microgels (**MM + FITC-PEI**) with the Rho-Gel photopatterned bulky hydrogel. (b) Schematic illustration of an MSA with PEI and gelatin photoligated hydrogel cuboids. (c) Pieces of PEI-ligated hydrogels (blue, P-GEL) and gelatin-ligated hydrogels (red, G-GEL) were mixed and shaken in water, resulting in a self-assembled structure. (d) The blank hydrogels (yellow) without any modification do not participate in the self-assembly. The scale bars in (c) and (d) are 1.5 cm. (e) Observation of the MSA hydrogel interface, hydrogels photoligated with FITC-PEI and Rho-Gel were used, which exhibit green and red fluorescence, respectively.

The photosensitive hydrogels were prepared by crosslinking **MNB** (0.04 M) with acrylamide (AAm, 2 M) and N,N'-methylene-bisacrylamide (MBA, 0.02 mM) in an acetonitrile–water solution (1/4, v/v) that was initiated by the redox pair of ammonium peroxodisulfate (APS) and N,N,N',N'-tetramethylethylenediamine (TEMED). After removing the unreacted monomers and initiators by washing, millimetre scale hydrogel units were obtained by cutting the bulky hydrogels. Polycationic PEI (M_w = 70 000) and electronegative gelatin (PI value = 4.7) were selected as the amino-containing macromolecules for photoligation on the hydrogel surface, and the morphologies of the freeze-dried hydrogel surface were observed using scanning electron microscopy (SEM) (Fig. S6, see the ESI†). Compared to the rugged network structure of the unmodified xerogel, the gelatin or PEI modified xerogels exhibited fibre-like networks with reduced surface roughness. In order to further demonstrate that amino-containing polyelectrolytes can be photoligated to the surface of the hydrogels, we prepared **MNB** containing microgels ($\sim$640 nm in diameter) and explored the evolution of the surface zeta potential after photoligation (as illustrated in Fig. 1a). Fig. 1b shows that the surface zeta potential (ζ) of the microgels changes from 0.8 mV to 7.2 mV and then −5.0 mV after the photoligation of PEI and the subsequent gelatin adsorption, correspondingly. The second charge reversal indicates that the photoligated polyelectrolytes keep their ability to adsorb macromolecules with opposite charges *via* electrostatic interactions.

Based on the successful photoligation and the retention for further supramolecular interactions, we first explored the MSA between microgels and a bulky hydrogel. As illustrated in Fig. 2a, rhodamine labelled gelatin (Rho-Gel, red) was photopatterned on a bulky hydrogel (10 × 10 × 3 mm, $l \times w \times h$) using a chrome photomask with a 400 μm width line, and fluorescein isothiocyanate labelled PEI (FITC-PEI, green) was photopatterned on the surface of the microgels (MM + FITC-PEI). To visualize the bulky hydrogel, we also photoimmobilized coumarin labelled BSA (blue) in the other regions of the bulky hydrogel. After shaking the bulky
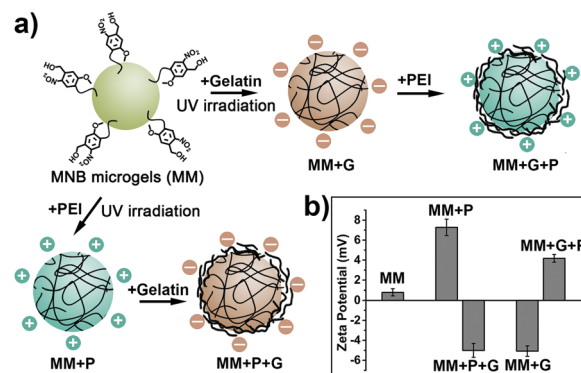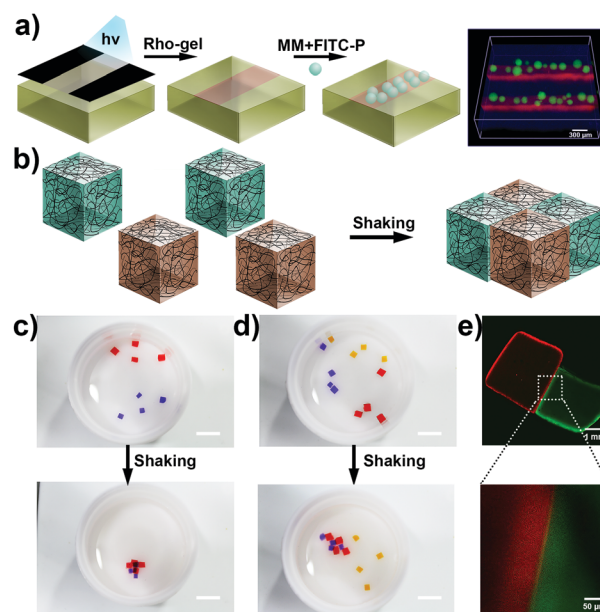
hydrogel and microgels in water (120 rpm), it was found that all microgels assemble in the patterned lines of the hydrogel, showing spatially controllable MSAs induced by electrostatic interactions. Then, the millimetre-level MSA was explored using cuboid hydrogel pieces (4 × 4 × 3 mm, $l \times w \times h$) that were stained using water-soluble dyes for visualization. As shown in Fig. 2b and c, mixing of the PEI-ligated hydrogels (blue, P-GEL) and gelatin-ligated hydrogels (red, G-GEL), followed by agitation (120 rpm) in water, permits

the binding of two kinds of hydrogels to form a combined gel with alternating assembled structures (Movie S1, see the ESI†). In a control experiment as shown in Fig. 2d, the blank hydrogel (yellow) did not stick to the P-GEL and G-GEL (Movie S2, see the ESI†). Moreover, no homogeneous assembly of P-GEL/P-GEL or G-GEL/ G-GEL was found. Fig. 2e shows the fluorescence images of MSA hydrogels photoligated with FITC-PEI and Rho-Gel, respectively, which exhibit uniform surface modification and tight contact at the self-assembled hydrogel interface. In addition, other proteins with different PI values were also photoligated on hydrogels as well as gelatin, and their probability of forming an MSA with P-GEL was investigated (Table S1, see the ESI†). The results exhibit that the MSA probability of hydrogels is greatly dependent on the PI value of the protein, which is consistent with the strength of the electrostatic interaction. These results suggests that electrostatic interaction plays an important role not only on the molecular level, but also on the macroscopic level.

Based on the spatial controllable advantage of light, the hydrogel cuboids are expected to realize precise MSAs *via* photopatterning technology. The arbitrary photopatterning of PEI and gelatin to hydrogels have been proven using photo-masks with different patterns (Fig. S7, see the ESI†), which means **MNB** functionalized hydrogels can achieve precise, controllable surface modification. When PEI and gelation were photopatterned on a single face of the hydrogel cuboids, as illustrated in Fig. 3a, a face specific self-assembly formed and dimer structures were obtained after random shaking in water (Movie S3, see the ESI†). On further photopatterning of PEI (blue) or gelatin (red) on the opposite faces of the hydrogel cuboids, a linear chain structure containing alternative red and blue hydrogel cuboids was formed as expected (Movie S4, see the ESI†). Finally, a more complex MSA system was designed. As illustrated in Fig. 3c, gelatin was photopatterned on the notched surface of the big cylindrical hydrogels (red), and PEI was modified on the side of the small cylindrical hydrogels (blue) that formed complementary structures with notches of gelatin patterned hydrogels. After random shaking in water, two assembled structures of teddy bear heads were formed through structural matching and surface electrostatic interaction. Noticeably, the interaction between PEI and gelatin photopatterned hydrogels is strong enough to support the stability of the self-assembled structures, which can be removed from the water without any disintegration (inset figures in Fig. 3b and c). Moreover, the assembled hydrogels can maintain the normal operation of an LED in a DC circuit after the incorporation of conductive graphene (Fig. S8, see the ESI†).

As it has been reported that MSA behaviour is often influenced by the mechanical strength of the substrates,[16] we explored the effect of elastic modulus on the MSAs of the hydrogels. The modulus of the hydrogel cuboids was adjusted by only changing the content of the cross-linker MBA (from 0.02 mM to 0.08 mM). As listed in Table 1, the synthesized hydrogels show different moduli and the value of G' increases from 548.0 Pa to 1782.4 Pa with increasing MBA content (Fig. S9, see the ESI†). After photo-ligation with PEI and gelatin, MSA investigation shows that
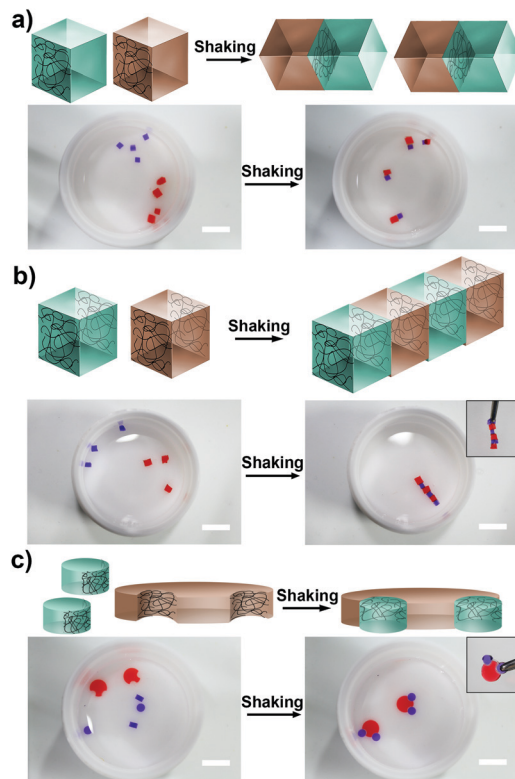

Fig. 3 MSA of photopatterned hydrogels. (a) Self-assembled dimers using single-face photopatterned hydrogels. (b) Alternating self-assembled chains were formed in accordance with the complementary photopat-terning in opposite faces of the hydrogels. (c) Self-assembled teddy bear head structure by complementary photopatterning. PEI photopatterned hydrogels were stained in blue and gelatin photopatterned hydrogels were stained in red. The scale bars are 1.5 cm.

hydrogels containing 0.02–0.06 mM MBA can self-assemble effec-tively, while the hydrogels containing 0.08 mM MBA have difficulty forming stable MSA structures. Moreover, the hydrogels without complementary electrostatic interaction can't self-assemble. After comparing the fracture tension stress of the self-assembled hydro-gels (Fig. S10, see the ESI†), it was indicated that the hydrogels with lower moduli are advantageous for the formation of electrostatic-induced MSAs, in which the hydrogels containing 0.02 mM MBA have the highest *in situ* interactive force with a fracture stress of 521.1 ± 3.7 Pa.

Table 1 Properties of MSA of millimeter scale hydrogels

MBA (mM)	$G'{}^a$ (Pa)	$G'{}^a$ (Pa)	PEI	Gelatin	Assembly[b]	Stress (Pa)	Strain (%)
0.08	1782.4	474.0	+	+	N	—	—
0.06	1165.8	355.7	+	+	A	95.1 ± 1.3	32.2 ± 1.3
0.04	796.7	119.9	+	+	A	221.5 ± 3.2	35.8 ± 1.4
0.02	548.0	39.2	+	+	A	521.1 ± 3.7	38.7 ± 1.6
0.02	548.0	39.2	+	−	N	—	—
0.02	548.0	39.2	−	+	N	—	—

[a] Values were determined at 1 Hz; "+" means hydrogels with PEI/gelatin photoligation; "−" means unmodified hydrogels. [b] A: assembling, N: no assembling.

In summary, we have successfully constructed millimetre-level precise supramolecular architectures. The photoligation chemistry of **MNB** enables PEI and gelatin polyelectrolytes to be modified on the surface of hydrogels, thereby realizing MSAs of hydrogels through surface electrostatic interactions. Due to the spatial controllability of photopatterning, precise MSAs with different architectures can be designed and implemented, such as dimers, linear chains and teddy bear heads. We expect that this surface photopatterning strategy is applicable to specific interactions with components that have host–guest molecular recognition, which provides a new potential strategy for the construction of ordered scaffolds in tissue engineering.

C. Bao proposed and supervised the project. Y. Xue, K. Ye, X. Wang, Y. Xiang carried out the synthesis, characterizations and data collection. C. Bao and L. Zhu oversaw the preparation of the paper with edits from all authors. All the authors discussed the results and commented on the manuscript.

Conflicts of interest

There are no conflicts to declare.

Notes and references

1 (a) N. B. Bowden, M. Weck, I. S. Choi and G. M. Whitesides, *Acc. Chem. Res.*, 2001, **34**, 231–238; (b) A. Harada, R. Kobayashi, Y. Takashima, A. Hashidzume and H. Yamaguchi, *Nat. Chem.*, 2011, **3**, 34–37; (c) M.-J. Cheng, Q. Zhang and F. Shi, *Chin. J. Polym. Sci.*, 2018, **36**, 306–321.

2 (a) D. H. Gracias, J. T. Tien, T. L. Breen, C. Hsu and G. M. Whitesides, *Science*, 2000, **289**, 1170–1172; (b) Q. Li, Y.-W. Zhang, C.-F. Wang, D. A. Weitz and S. Chen, *Adv. Mater.*, 2018, **30**, 1803475; (c) Z. Yu, J. Liu, C. S. Y. Tan, O. A. Scherman and C. Abell, *Angew. Chem., Int. Ed.*, 2018, **57**, 3079–3083.

3 (a) T. Kakuta, Y. Takashima, T. Sano, T. Nakamura, Y. Kobayashi, H. Yamaguchi and A. Harada, *Macromolecules*, 2015, **48**, 732–738; (b) S. Tamesue, K. Yasuda and T. Endo, *ACS Appl. Mater. Interfaces*, 2018, **10**, 29925–29932.

4 (a) C. Wang, C. Lin, R. Ming, X. Li, P. Jonkheijm, M. Cheng and F. Shi, *ACS Appl. Mater. Interfaces*, 2021, **13**, 28774–28781; (b) S. Tasoglu, D. Kavaz, U. A. Gurkan, S. Guven, P. Chen, R. Zheng and U. Demirci, *Adv. Mater.*, 2013, **25**, 1137–1143.

5 (a) Q. Zhang, Y. Sun, C. He, F. Shi and M. Cheng, *Adv. Sci.*, 2020, **7**, 2002025; (b) M. Cheng, G. Zhu, L. Li, S. Zhang, D. Zhang, A. J. C. Kuehne and F. Shi, *Angew. Chem., Int. Ed.*, 2018, **57**, 14106–14110; (c) J. Li, Z. Xu, Y. Xiao, G. Gao, J. Chen, J. Yin and J. Fu, *J. Mater. Chem. B*, 2018, **6**, 257–264.

6 (a) H. Yamaguchi, Y. Kobayashi, R. Kobayashi, Y. Takashima, A. Hashidzume and A. Harada., *Nat. Commun.*, 2012, **3**, 603; (b) Y. Zeng, Y. Kobayashi, T. Sekine, Y. Takashima, A. Hashidzume, H. Yamaguchi and A. Harada, *Commun. Chem.*, 2018, **1**, 4; (c) Q.-J. Yuan, Y.-F. Wang, J.-H. Li, B.-J. Li and S. Zhang, *Macromol. Rapid Commun.*, 2013, **34**, 1174–1180; (d) T. Itami, A. Hashidzume, Y. Kamon, H. Yamaguchi and A. Harada, *Sci. Rep.*, 2021, **11**, 6320.

7 (a) L. Wang, M. Qiu, Q. Yang, Y. Li, G. Huang, M. Lin, T. J. Lu and F. Xu, *ACS Appl. Mater. Interfaces*, 2015, **7**, 11134–11140; (b) N. B. Bowden, M. Weck, I. S. Choi and G. M. Whitesides, *Acc. Chem. Res.*, 2001, **34**, 231–238.

8 (a) S.-M. Kang, C.-H. Choi, J. Kim, S.-J. Yeom, D. Lee, B. J. Parkc and C.-S. Lee, *Soft Matter*, 2016, **12**, 5847–5853; (b) S. Tasoglu, D. Kavaz, U. A. Gurkan, S. Guven, P. Chen, R. Zheng and U. Demirci, *Adv. Mater.*, 2013, **25**, 1137–1143; (c) Y. Kobayashi, Y. Takashima, A. Hashidzume, H. Yamaguchi and A. Harada, *Sci. Rep.*, 2013, **3**, 1243; (d) M. Nakahata, Y. Takashima, A. Hashidzume and A. Harada, *Chem. – Eur. J.*, 2014, **21**, 2770–2774.

9 M. Cheng and F. Shi, *Chem. – Eur. J.*, 2020, **26**, 15763–15778.

10 G. Ju, F. Guo, Q. Zhang, A. J. C. Kuehne, S. Cui, M. Cheng and F. Shi, *Adv. Mater.*, 2017, **29**, 1702444.

11 (a) Q. Li, Y.-W. Zhang, C.-F. Wang, D. A. Weitz and S. Chen, *Adv. Mater.*, 2018, **30**, 1803475; (b) S. Tasoglu, D. Kavaz, U. A. Gurkan, S. Guven, P. Chen, R. Zheng and U. Demirci, *Adv. Mater.*, 2013, **25**, 1137–1143.

12 (a) S. E. Chung, X. Dong and M. Sitti, *Lab Chip*, 2015, **15**, 1667–1676; (b) S. K. Y. Tang, R. Derda, A. D. Mazzeo and G. M. Whitesides, *Adv. Mater.*, 2011, **23**, 2413–2418.

13 H. Qi, M. Ghodousi, Y. Du, C. Grun, H. Bae, P. Yin and A. Khademhosseini, *Nat. Commun.*, 2013, **4**, 2275.

14 (a) Z. Ming, J. Fan, C. Bao, Y. Xue, Q. Lin and L. Zhu, *Adv. Funct. Mater.*, 2018, **28**, 1706918; (b) Y. Xue, D. Liu, C. Wang, C. Bao, X. Wang, H. Zhu, H. Mao, Z. Cai, Q. Lin and L. Zhu, *ACS Appl. Bio Mater.*, 2020, **3**, 2410–2418; (c) J. C. Grim, T. E. Brown, B. A. Aguado, D. A. Chapnick, A. L. Viert, X. Liu and K. S. Anseth, *ACS Cent. Sci.*, 2018, **4**, 909–916; (d) T. E. Brown and K. S. Anseth, *Chem. Soc. Rev.*, 2017, **46**, 6532–6552.

15 C. Wang, Y. Liu, C. Bao, Y. Xue, Y. Zhou, D. Zhang, Q. Lin and L. Zhu, *Chem. Commun.*, 2020, **56**, 2264–2267.

16 G. Ju, M. Cheng, F. Guo, Q. Zhang and F. Shi, *Angew. Chem., Int. Ed.*, 2018, **57**, 8963–8967.